Realistic Earth matter effects and a method to acquire information about small θ_{13} in the detection of supernova neutrinos

Xin-Heng Guo,[1,*] Ming-Yang Huang,[1,†] and Bing-Lin Young[2,3,‡]

[1]*College of Nuclear Science and Technology, Beijing Normal University, Beijing 100875, China*
[2]*Department of Physics and Astronomy, Iowa State University, Ames, Iowa 5001, USA*
[3]*Institute of Theoretical Physics, Chinese Academy of Sciences, Beijing, China*

(Received 12 November 2008; published 18 June 2009)

In this paper, we first calculate the realistic Earth matter effects in the detection of type II supernova neutrinos at the Daya Bay reactor neutrino experiment which is currently under construction. It is found that the Earth matter effects depend on the neutrino incident angle θ, the neutrino mass hierarchy Δm^2_{31}, the crossing probability at the high resonance region inside the supernova, P_H, the neutrino temperature, T_α, and the pinching parameter in the neutrino spectrum, η_α. We also take into account the collective effects due to neutrino-neutrino interactions inside the supernova. With the expression for the dependence of P_H on the neutrino mixing-angle θ_{13}, we obtain the relations between θ_{13} and the event numbers for various reaction channels of supernova neutrinos. Using these relations, we propose a possible method to acquire information about θ_{13} smaller than 1.5°. Such a sensitivity cannot be achieved by the reactor neutrino deta at the Daya Bay experiment which has a sensitivity of the order of $\theta_{13} \sim 3°$. Furthermore, we apply this method to other neutrino experiments, i.e. Super-K, SNO, KamLAND, LVD, MinBooNE, Borexino, and Double-Chooz. We also study the energy spectra of the differential event numbers, dN/dE.

DOI: 10.1103/PhysRevD.79.113007 PACS numbers: 14.60.Pq, 13.15.+g, 25.30.Pt, 26.30.−k

I. INTRODUCTION

Observable effects of supernova (SN) neutrinos in underground detectors have been a subject of intense investigation in astroparticle physics, both on general grounds and in relation to the SN event like 1987A [1]. In particular, flavor oscillation in SN may shed light on the problem of neutrino masses and mixing by means of the associated matter effects. Several neutrino laboratories, including the Daya Bay reactor neutrino underground laboratory [2] which is under construction, can be used to detect possible neutrino events from an SN explosion and serve as the SN Earth Warning System [3]. Hence theoretical prediction for the detection of SN neutrinos in the Daya Bay and other neutrino experiments is very desirable.

In Ref. [4], the authors studied the matter effects, including both the Earth and SN, on the detection of neutrinos from a type II SN explosion. The results of the study were applied to the Daya Bay reactor neutrino experiment which measures the mixing-angle θ_{13} down to $\sin^2 2\theta_{13} = 0.01$. In that paper, a simplified picture for the matter density of the Earth was used, i.e. the mantle-core-mantle picture in which $\rho = 12\ \mathrm{g/cm^3}$ (ρ is the Earth matter density) for the core and $\rho = 5\ \mathrm{g/cm^3}$ for the mantle, where the core radius and the thickness of the mantle are half of the Earth radius, respectively. The energy spectra of neutrinos from the cooling stage were assumed as exactly thermal and the average temperature for the neutrinos, $T_{\nu_e} = 3.5$ MeV, $T_{\bar{\nu}_e} = 5$ MeV, and $T_{\nu_x} = 8$ MeV, were used (ν_x denotes ν_μ, $\bar{\nu}_\mu$, ν_τ, or $\bar{\nu}_\tau$). Because of the large mixing-angle solution of neutrinos [5], the crossing probability at the low resonance region inside the SN, P_L, is zero. Since the crossing probability at the high resonance region, P_H, depends on the unknown neutrino mixing-angle θ_{13}, two extreme cases, i.e. P_H being 0 and 1, were studied. In the present work, we improve the investigation in Ref. [4] by generalizing the simplified mantle-core-mantle picture for the Earth matter density to the realistic density profile including the effects due to variations of the neutrino temperature T_α and the pinching parameter η_α in the neutrino energy spectra. We also include the collective effects arising from neutrino-neutrino interactions in the SN. Furthermore, the target material is taken to be the Linear Alkyl Benzene (LAB), which has been selected as the main part of the liquid scintillator in the Daya Bay experiment [2], instead of C_9H_{12} as used in Ref. [4].

In the realistic case, the matter density of the Earth changes with the depth continuously [6], the energy spectra of neutrinos from the cooling stage are not exactly thermal and has a nonvanishing pinching parameter, and the neutrino temperature may vary in some ranges [5,7,8]. Furthermore, since neutrino and antineutrino densities are very high near the neutrinosphere, the neutrino-neutrino interactions become significant. This leads to collective effects in the SN which affect the neutrino spectra [9–16]. One main purpose of the present work is to investigate the effects of all these factors on the detection of SN neutrinos. In order to compare with Ref. [4], we will first calculate the effects of the realistic distribution of the Earth

*xhguo@bnu.edu.cn
†Corresponding author: hmy19151905@mail.bnu.edu.cn
‡young@iastate.edu

matter density on the detection of SN neutrinos in the simple case $T_{\nu_e} = 3.5$ MeV, $T_{\bar{\nu}_e} = 5$ MeV, and $T_x = 8$ MeV, in the absence of pinching parameters, i.e., $\eta_{\nu_e} = \eta_{\bar{\nu}_e} = \eta_{\nu_x} = 0$. Then we study the effects due to the variation of neutrino temperatures and the inclusion of the pinching parameters in the energy spectra. In the future, if the values of T_α and η_α can be constrained more precisely, the event number of SN neutrinos can be more accurately predicted.

The other main purpose of the present paper is to propose a possible method to acquire information about θ_{13} below the sensitivity of the Daya Bay experiment, i.e. 3°, through the detection of SN neutrinos. This can be achieved since at the high resonance region inside the SN, the crossing probability P_H is very sensitive to θ_{13}. Analytical expressions for transition probabilities between different neutrino flavors have been investigated in the literatures. Using the Landau-Zener formula [17], the crossing probability, P_C, which is the neutrino jumping probability from one mass eigenstate to another at the resonance region, were also calculated for specific matter density distributions, including the linear [18–21], exponential [22], hyperbolic tangent [23], and $1/r$ [24,25] density distributions. Using a similar method, the crossing probabilities at the high and low resonance regions inside the SN, P_H and P_L, were given in [25–27]. The neutrino event numbers N which we will obtain depend on P_H. Using the relation between P_H and θ_{13}, we can predict the SN neutrino event numbers N as a function of θ_{13}. With this, we give a possible method to acquire information about θ_{13} smaller than 1.5° by measuring the ratios of the event numbers of different flavor of SN neutrinos, e.g., the ratio of the event numbers of ν_e and $\bar{\nu}_e$. This method is applied to the existing neutrino experiments and experiments under construction, including Daya Bay, Super-K, SNO, KamLAND, LVD, MinBooNE, Borexino, and Double-Chooz.

Finally, the energy spectra of the differential neutrino event numbers, dN/dE, where E is the neutrino energy, will be studied. We will make predictions for dN/dE as a function of E for different neutrino Earth incident angles θ and for different values of θ_{13}. Then we discuss some interesting properties of these predictions.

The paper is organized as follows. In Sec. II, we review the necessary formulas for the detection of SN neutrinos on the Earth. In Sec. III, we apply these formulas to the Daya Bay experiment, where the realistic Earth matter density, the collective effects, the variation of the neutrino temperature, and the pinching of the neutrino spectra are considered. In Sec. IV, the relation between the neutrino event number N and θ_{13} is discussed and a method to obtain information about θ_{13} smaller than 1.5° is proposed. This method is applied to the Daya Bay experiment as an explicit example. In Sec. V, the method is applied to several existing main neutrino experiments, including Super-K, SNO, KamLAND, LVD, MinBooNE, Borexino, and another experiment under construction Double-Chooz. In Sec. VI, we study the energy spectra of the differential neutrino event numbers (dN/dE) and discuss some of their properties. Finally, a summary is given in the concluding Sec. VII.

II. FORMULAS FOR DETECTION OF SN NEUTRINOS ON THE EARTH

The SN explosion is one of the most spectacular cosmic events and a source of new physical ideas. A broad area of topics of fundamental physics can be studied by the observation of SN. In the core collapse of SN, a vast amount of neutrinos are produced in two bursts. In the first burst which lasts for only a few milliseconds, electron neutrinos are generated via the inverse beta-decay process which leads to a neutron rich star. In the second burst which lasts longer, neutrinos of all flavors are produced via the nucleon-nucleon bremsstrahlung process, $\nu_e\bar{\nu}_e$ annihilation, and e^+e^- annihilation [28–30].

When the SN neutrinos of each flavor are produced they are approximately the effective mass eigenstates due to the extremely high matter density environment. While they propagate outward to the surface of the SN they could experience collective effects arising from neutrino-neutrino interactions [9–16] and the well-known Mikheyev-Smirnov-Wolfenstein (MSW) effects [18–25]. After travelling the cosmic distance to reach the Earth, the arriving neutrinos are mass eigenstates, which then oscillate in flavors while going through the Earth matter. Therefore, we also have to consider the Earth matter effects [4,5,31–33] when we compute the event numbers of the various flavors of neutrions.

In the Daya Bay experiment, SN neutrinos undergo the following reactions in the detector.

(1) $\bar{\nu}_e + p$ reaction

The large cross section, low threshold, and abundance of target protons make this the dominant channel for the detection of SN neutrinos. The inverse beta-decay process,

$$\bar{\nu}_e + p \rightarrow e^+ + n,$$

has a reaction threshold [34,35]

$$E_{\text{th}} = 1.80 \text{ MeV}. \tag{1}$$

At low energies we approximate the large cross section as [35,36]

$$\sigma(\bar{\nu}_e p) = 9.5 \times 10^{-44}(E(\text{MeV}) - 1.29)^2 \text{ cm}^2. \tag{2}$$

(2) $\nu - e^-$ scattering

The neutrino-electron scattering,

$$\begin{aligned}
&\nu_e + e^- \to \nu_e + e^- \qquad \text{(CC and NC)},\\
&\bar{\nu}_e + e^- \to \bar{\nu}_e + e^- \qquad \text{(CC and NC)},\\
&\nu_\alpha + e^- \to \nu_\alpha + e^- \qquad \text{(NC)},\\
&\bar{\nu}_\alpha + e^- \to \bar{\nu}_\alpha + e^- \qquad \text{(NC)}, \qquad \alpha = \mu, \tau
\end{aligned}$$

where CC and NC stand, respectively, for the changed current and neutral current interactions, produce recoil electrons with energy from zero up to the kinematics maximum. In our rate calculation we integrate over the ranges of the electron recoil energies. Then, the total cross sections for the neutrino-electron scattering are linearly proportional to the neutrino energy, and have the following forms [35]:

$$\begin{aligned}
\sigma(\nu_e e \to \nu_e e) &= 9.20 \times 10^{-45} E(\text{MeV})\ \text{cm}^2,\\
\sigma(\bar{\nu}_e e \to \bar{\nu}_e e) &= 3.83 \times 10^{-45} E(\text{MeV})\ \text{cm}^2,\\
\sigma(\nu_{\mu,\tau} e \to \nu_{\mu,\tau} e) &= 1.57 \times 10^{-45} E(\text{MeV})\ \text{cm}^2,\\
\sigma(\bar{\nu}_{\mu,\tau} e \to \bar{\nu}_{\mu,\tau} e) &= 1.29 \times 10^{-45} E(\text{MeV})\ \text{cm}^2.
\end{aligned} \tag{3}$$

(3) ^{12}C reactions

For the neutrinos and ^{12}C system, there are two charged-current and six neutral-current reactions. The effective cross sections are obtained by scaling the experimentally measured energy values from the decay of the muon at rest to the energy scale for SN neutrinos. In this way, one can obtain the following effective cross sections [35–37]:

Charged-current capture of $\bar{\nu}_e$:

$$\begin{aligned}
\bar{\nu}_e + {}^{12}\text{C} &\to {}^{12}\text{B} + e^+,\\
E_{\text{th}} &= 14.39\ \text{MeV},\\
{}^{12}\text{B} &\to {}^{12}\text{C} + e^- + \bar{\nu}_e,\\
\langle\sigma({}^{12}\text{C}(\bar{\nu}_e, e^+){}^{12}\text{B})\rangle &= 1.87 \times 10^{-42}\ \text{cm}^2.
\end{aligned} \tag{4}$$

Charged-current capture of ν_e:

$$\begin{aligned}
\nu_e + {}^{12}\text{C} &\to {}^{12}\text{N} + e^-,\\
E_{\text{th}} &= 17.34\ \text{MeV},\\
{}^{12}\text{N} &\to {}^{12}\text{C} + e^+ + \nu_e,\\
\langle\sigma({}^{12}\text{C}(\nu_e, e^-){}^{12}\text{N})\rangle &= 1.85 \times 10^{-43}\ \text{cm}^2.
\end{aligned} \tag{5}$$

Neutral-current inelastic scattering of ν_α or $\bar{\nu}_\alpha$ where $\alpha = e, \mu, \tau$:

$$\begin{aligned}
\nu_\alpha + {}^{12}\text{C} &\to {}^{12}\text{C}^* + \nu'_\alpha, \qquad E_{\text{th}} = 15.11\ \text{MeV},\\
\bar{\nu}_\alpha + {}^{12}\text{C} &\to {}^{12}\text{C}^* + \bar{\nu}'_\alpha, \qquad E_{\text{th}} = 15.11\ \text{MeV},\\
{}^{12}\text{C}^* &\to {}^{12}\text{C} + \gamma,\\
\langle\sigma(\nu_e {}^{12}\text{C})\rangle &= 1.33 \times 10^{-43}\ \text{cm}^2,\\
\langle\sigma(\bar{\nu}_e {}^{12}\text{C})\rangle &= 6.88 \times 10^{-43}\ \text{cm}^2,\\
\langle\sigma(\nu_x(\bar{\nu}_x){}^{12}\text{C})\rangle &= 3.73 \times 10^{-42}\ \text{cm}^2, \qquad x = \mu, \tau.
\end{aligned} \tag{6}$$

The effective cross sections in Eqs. (4)–(6) are given for SN neutrinos without oscillations [4,35]. When neutrino oscillations are taken into account, the oscillations of higher energy ν_x into ν_e result in an increased event rate since the expected ν_e energies are just at or below the charged-current reaction threshold. This leads to an increase by a factor of 35 for the cross section $\langle\sigma({}^{12}\text{C}(\nu_e, e^-){}^{12}\text{N})\rangle$ if we average it over a ν_e distribution with $T = 8$ MeV rather than 3.5 MeV. Similarly, the cross section $\langle\sigma({}^{12}\text{C}(\bar{\nu}_e, e^+){}^{12}\text{B})\rangle$ is increased by a factor of 5. For the case of neutral-current inelastic scattering of ν_α or $\bar{\nu}_\alpha$, when the oscillations of higher energy ν_x into ν_e and $\bar{\nu}_x$ into $\bar{\nu}_e$ are taken into account, the cross section $\langle\sigma(\nu_e {}^{12}\text{C})\rangle$ is increased by a factor of 28 and the cross section $\langle\sigma(\bar{\nu}_e {}^{12}\text{C})$ is increased by a factor of 5.

There will be several detectors located at the near and far sites at the Daya Bay experiment. In Ref. [4], the authors take the liquid scintillator to be mainly C_9H_{12} and the total detector mass to be 300 tons. The Daya Bay Collaboration has decided to use LAB as the main part of the liquid scintillator and the total detector mass is about 300 tons. LAB, which has a chemical composition including C and H, is a mixture of the monoalkyl benzene with 9 to 14 carbon atoms in the side chain. The main LAB components contain 10 to 13 carbon atoms in the side chain. Therefore, LAB can be approximately expressed as $C_6H_5 - C_nH_{2n+1}$ where $n = 9 \sim 14$. In our calculation, the ratio of the numbers of C and H, N_C/N_H, is about 0.6. Then the total numbers of target protons, electrons, and ^{12}C are

$$N_T^{(p)} = 2.20 \times 10^{31}, \qquad N_T^{(e)} = 1.01 \times 10^{32}, \qquad N_T^{(C)} = 1.32 \times 10^{31}. \tag{7}$$

Neutrinos from an SN may travel through a significant portion of the Earth before reaching the detector and are therefore subject to the Earth matter effects. Suppose a neutrino reaches the detector with the incident angle θ as indicated in Fig. 1, then the distance the neutrino travelling through the Earth is

$$L = (-R + h)\cos\theta + \sqrt{R^2 - (R - h)^2 \sin^2\theta}, \tag{8}$$

where h is the underground depth of the detector and R (6400 km) is the radius of the Earth. At the Daya Bay

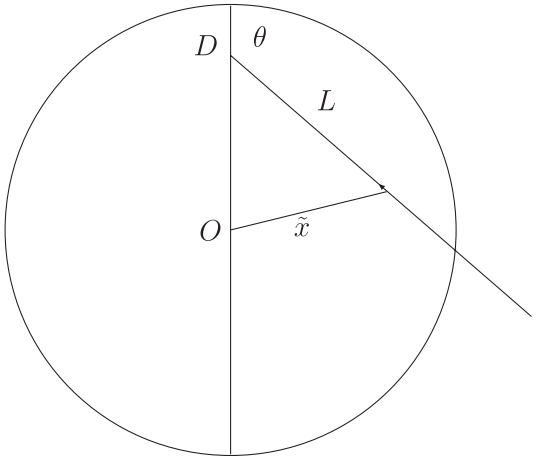

FIG. 1. Illustration of the path of the SN neutrino reaching the detector in the Earth. D is the location of the detector, θ is the incident angle of the neutrino, O is the center of the Earth, L is the distance the neutrino travels through the Earth, and $\tilde{x}$ is the distance of the neutrino to the center of the Earth.

experiment, $h \approx 0.4$ km. Let x be the distance that the neutrino travels into the Earth, then the distance of the neutrino to the center of the Earth, $\tilde{x}$, is given by

$$\tilde{x} = \sqrt{(-R + h)^2 + (L - x)^2 + 2(R - h)(L - x)\cos\theta}. \tag{9}$$

In the following, we will calculate the event numbers of SN neutrinos that can be observed through various reaction channels "i" at the Daya Bay experiment. This will be done by integrating over the neutrino energy E, the product of the target number N_T, the cross section of each channel σ, and the neutrino flux function $F_\alpha^D(E)/4\pi D^2$,

$$N_\alpha(i) = N_T \int dE \cdot \sigma(i) \cdot \frac{1}{4\pi D^2} \cdot F_\alpha^D, \tag{10}$$

where α stands for the neutrino or antineutrino of a given flavor, D is the distance between the SN and the Earth, and the index i represents different channels through which SN neutrinos are observed.

For the neutrino of flavor α, the time-integrated neutrino energy spectra can be described by the Fermi-Dirac distribution (we consider the case where the spectra of neutrinos from the cooling stage are not exactly thermal) [5,7,8,28,38],

$$F_\alpha^{(0)}(E) = \frac{N_\alpha^{(0)}}{F_{\alpha 2} T_\alpha^3} \frac{E^2}{\exp(E/T_\alpha - \eta_\alpha) + 1}, \tag{11}$$

where T_α is the typical temperature of the neutrino [5,7,8],

$$\begin{aligned} &T_{\nu_e} = 3\text{–}4 \text{ MeV}, \qquad T_{\bar{\nu}_e} = 5\text{–}6 \text{ MeV}, \\ &T_{\nu_x} = 7\text{–}9 \text{ MeV}, \qquad (\nu_x = \nu_\mu, \nu_\tau, \bar{\nu}_\mu, \bar{\nu}_\tau), \end{aligned} \tag{12}$$

and η_α is the pinching parameter of the spectra ($\eta_\alpha > 0$) to represent the deviation from being exactly thermal. The values of η_α for ν_x and $\bar{\nu}_x$ ($x = \mu, \tau$) are the same (which will be denoted as η_{ν_x} in the following) since they have the same interactions, and are in general different from η_{ν_e} or $\eta_{\bar{\nu}_e}$. The values of η_α need not be constant throughout the cooling stage, and are typically [5,7,8]

$$\begin{aligned} &\eta_{\nu_e} \approx 3\text{–}5, \qquad \eta_{\bar{\nu}_e} \approx 2.0\text{–}2.5, \qquad \eta_{\nu_x} \approx 0\text{–}2, \\ &(\nu_x = \nu_\mu, \nu_\tau, \bar{\nu}_\mu, \bar{\nu}_\tau). \end{aligned} \tag{13}$$

In Eq. (11), $F_{\alpha j}$, where j is an integer, is defined by

$$F_{\alpha j} = \int_0^\infty \frac{x^j}{\exp(x - \eta_\alpha) + 1} dx, \tag{14}$$

and $N_\alpha^{(0)}$ is the total number of the neutrinos of flavor α,

$$N_\alpha^{(0)} = \frac{L_\alpha^{(0)}}{\langle E_\alpha^{(0)} \rangle}, \tag{15}$$

where the average neutrino energy is $\langle E_\alpha^{(0)} \rangle = \frac{F_{\alpha 3}}{F_{\alpha_2}} T_\alpha$ and the luminosity $L_\alpha^{(0)}$ is related to the total energy release during the SN explosion, $E_{SN}^{(0)}$, through the following equation:

$$L_\alpha^{(0)} = \frac{0.99}{6} E_{SN}^{(0)}. \tag{16}$$

In the numerical calculations below we take

$$E_{\text{SN}}^{(0)} = 1.97 \times 10^{59} \text{ MeV}, \tag{17}$$

and the distance D to be 10 kpc $= 3.09 \times 10^{22}$ cm [39,40]. Using the above formulas, the energy spectrum function can be rewritten as

$$F_\alpha^{(0)}(E) = \frac{L_\alpha^{(0)}}{F_{\alpha 3} T_\alpha^4} \frac{E^2}{\exp(E/T_\alpha - \eta_\alpha) + 1}. \tag{18}$$

In order to obtain the neutrino energy spectrum function at the detector, the collective effects [9–16], the MSW effects [18–25], and the Earth matter effects [5,31–33] should be considered. Let P_H (P_L) be the crossing probability at the high (low) resonance regions inside the SN, $P_{\nu\nu}$ represent the collective effects of neutrino-neutrino interactions which is a stepwise flavor conversion probability of neutrino at a critical energy E_C, and P_{ie} ($i = 1, 2, 3$) be the probability that a neutrino mass eigenstate ν_i enters the surface of the Earth and arrives at the detector as an electron neutrino ν_e. Then the flux of ν_e at the detector, denoted as $F_{\nu_e}^D$, can be written as

$$F_{\nu_e}^D = \sum_i P_{ie} F_i, \tag{19}$$

where F_i is the flux of ν_i at the Earth surface, in either the normal or inverted hierarchy. P_{ie} is the probability of the ith mass eigenstate contained in ν_e and obeys the unitary condition $\sum_i P_{ie} = 1$.

A significant amount of studies on the collective effects of neutrino-neutrino interactions, including simulations, have been made by a number of authors, e.g., Duan *et al.* [9–11], Dusgupta *et al.* [12], Raffelt *et al.* [13,14], Esteban-Pretel *et al.* [15], and Fogli *et al.* [16]. In order to obtain a simple expression of the stepwise flavor conversion probabilities $P_{\nu\nu}$ for the neutrino and $\bar{P}_{\nu\nu}$ for the antineutrino, we take a constant matter density and box-spectra for both the neutrino and antineutrino [14]. An analysis of the collective effects in the case of three flavors has been made in [12], and it allows us to characterize the collective oscillation effects and to write down the flavor spectra of the neutrino and antineutrino arriving at the Earth. Following [12], we have $P_{\nu\nu} = \bar{P}_{\nu\nu} = 1$ in the case of normal hierarchy; while in the case of inverted hierarchy, one has $\bar{P}_{\nu\nu} = 1$, and

$$P_{\nu\nu} = \begin{cases} 1 & (E < E_C), \\ 0 & (E > E_C), \end{cases} \tag{20}$$

where $E_C = 7$ MeV [12,16].

Because of the large mixing-angle solution of the neutrino mixing, the crossing probability at the low resonance region inside the SN vanishes, $P_L = \bar{P}_L = 0$. Also, for very small $\sin\theta_{13}$, we can neglect the contributions from P_{3e} and $\bar{P}_{3e}$ [31]. Therefore, after a straightforward calculation the following results [12] for the fluxes at the detector can be obtained:

$$\begin{aligned} F_{\nu_e}^{D(N)} &= P_{2e}P_H F_{\nu_e}^{(0)} + (1 - P_{2e}P_H)F_{\nu_x}^{(0)}, \\ F_{\bar{\nu}_e}^{D(N)} &= (1 - \bar{P}_{2e})F_{\bar{\nu}_e}^{(0)} + \bar{P}_{2e}F_{\bar{\nu}_x}^{(0)}, \\ 2F_{\nu_x}^{D(N)} &= (1 - P_{2e}P_H)F_{\nu_e}^{(0)} + (1 + P_{2e}P_H)F_{\nu_x}^{(0)}, \\ 2F_{\bar{\nu}_x}^{D(N)} &= \bar{P}_{2e}F_{\bar{\nu}_e}^{(0)} + (2 - \bar{P}_{2e})F_{\bar{\nu}_x}^{(0)}, \end{aligned} \tag{21}$$

for the normal hierarchy ($\triangle m_{31}^2 > 0$), and

$$\begin{aligned} F_{\nu_e}^{D(I)} &= \begin{cases} P_{2e}F_{\nu_e}^{(0)} + (1 - P_{2e})F_{\nu_x}^{(0)}, & (E < E_C) \\ F_{\nu_x}^{(0)}, & (E > E_C) \end{cases} \\ F_{\bar{\nu}_e}^{D(I)} &= \bar{P}_H(1 - \bar{P}_{2e})F_{\bar{\nu}_e}^{(0)} + (1 + \bar{P}_{2e}\bar{P}_H - \bar{P}_H)F_{\bar{\nu}_x}^{(0)}, \\ 2F_{\nu_x}^{D(I)} &= \begin{cases} (1 - P_{2e})F_{\nu_e}^{(0)} + (1 + P_{2e})F_{\nu_x}^{(0)}, & (E < E_C) \\ F_{\nu_e}^{(0)} + F_{\nu_x}^{(0)}, & (E > E_C) \end{cases} \\ 2F_{\bar{\nu}_x}^{D(I)} &= (1 + \bar{P}_{2e}\bar{P}_H - \bar{P}_H)F_{\bar{\nu}_e}^{(0)} + (1 + \bar{P}_H - \bar{P}_{2e}\bar{P}_H)F_{\bar{\nu}_x}^{(0)}, \end{aligned} \tag{22}$$

for the inverted hierarchy ($\triangle m_{31}^2 < 0$).

Let us remark the important result that an unit flavor conversion probability means the absence of the collective effects. Hence as indicated in Eq. (21) the final SN neutrino and antineutrino fluxes in the normal hierarchy are not modified by the collective effects. Neither are the antineutrino fluxes in the inverted hierarchy. Only the neutrino fluxes in the inverted hierarchy and for $E > E_C$ are modified as indicated in Eq. (22).

The probability P_{ie} ($i = 1, 2, 3$) has been calculated in Ref. [31], in particular,

$$P_{2e} = \sin^2\theta_{12} + \frac{1}{2}\sin^2 2\theta_{12}\int_{x_0}^{x_f} dx V(x)\sin\phi_{x\to x_f}^m, \tag{23}$$

where $\theta_{12} = 32.5°$ [41], $V(x)$ is the potential that the neutrino experiences in the Earth, and $\phi_{a\to b}^m$ is defined as

$$\phi_{a\to b}^m = \int_a^b dx \triangle_m(x), \tag{24}$$

where

$$\triangle_m(x) = \frac{\triangle m_{21}^2}{2E}\sqrt{(\cos 2\theta_{12} - \varepsilon(x))^2 + \sin^2 2\theta_{12}}. \tag{25}$$

In Eq. (25), $\triangle m_{21}^2 = 7.1 \times 10^{-5}$ eV^2 and $\varepsilon(x)$ is defined as

$$\varepsilon(x) = \frac{2EV(x)}{\triangle m_{21}^2}. \tag{26}$$

For a typical neutrino energy $E = 10$ MeV, ε is less than 0.13 [4]. Therefore, we neglect contributions of $O(\varepsilon^2)$.

In the Earth the potential $V(x)$ is $\sqrt{2}G_F N_e(x)$ for an electron neutrino and $-\sqrt{2}G_F N_e(x)$ for an electron antineutrino where G_F is the Fermi constant and $N_e(x)$ is the electron number density in the Earth matter. Let the matter mass density inside the Earth be $\rho(x)$. For nuclei of equal number of protons and neutrons the electron number density is

$$N_e(x) = \rho(x)/(m_p + m_n), \tag{27}$$

where m_p and m_n are, respectively, the proton and neutron masses. The realistic matter density inside the Earth is shown in Table I [6].

Since the crossing probability at the high resonance region P_H depends on the neutrino mixing-angle θ_{13}, which is unknown [28,41,42], we will first consider two extreme cases, $P_H = 0$ (for the pure adiabatic conversion) and $P_H = 1$ (corresponding to a strong violation of the adiabatic condition). This enables us to estimate the range

TABLE I. The realistic matter density inside the Earth where r is the distance to the center of the Earth and $R = r(\text{km})/6371$ [6].

r (rm)	$\rho(10^3\ \text{kg}\cdot\text{m}^{-3})$
0–1221.5	$13.0885 - 8.8381R^2$
1221.5–3480.0	$12.5815 - 1.2638R - 3.6426R^2 - 5.5281R^3$
3480.0–5701.0	$7.9565 - 6.4761R + 5.5283R^2 - 3.0807R^3$
5701.0–5771.0	$5.3197 - 1.4836R$
5771.0–5971.0	$11.2494 - 8.0298R$
5971.0–6151.0	$7.1089 - 3.8045R$
6151.0–6346.6	$2.6910 + 0.6924R$
6346.6–6356.0	2.900
6356.0–6368.0	2.600
6368.0–6371.0	1.020

of the total neutrino event numbers to be given in Sec. III. Then in Sec. IV, we will obtain the expression of the crossing probability P_H and work out the relation between the event number N and θ_{13}. From appropriate ratios of event number which change with θ_{13}, we will be able to obtain some information about θ_{13} smaller than 1.5° by detecting SN neutrinos.

III. NUMERICAL RESULTS FOR EARTH MATTER EFFECTS IN THE DETECTION OF SN NEUTRINOS

In this section, we calculate the realistic Earth matter effects in the detection of type II SN neutrinos at the Daya Bay experiment and give the numerical results for the two extreme cases of $P_H = 1$ and 0. A summary of the results is given in Table II.

TABLE II. Summary of the realistic Earth matter effects. N (I) represents the normal (inverted) hierarchy, "1" ("0") represents $P_H = 1$ (0). The numbers in the columns 'Incipient' and 'Min' are the event numbers when the SN neutrino Earth incident angle is zero and is the angle in the column 'Angle', respectively. The column 'Angle' gives the angles at which the event numbers are minimum and the Earth matter effects are the strongest. The column 'Ratio' gives the percentages of the Earth matter effects.

Conditions	Hierarchy (P_H)	Reaction	Incipient	Min	Angle	Ratio
	$N(1)$	$\bar{\nu}_e p$	122.28	113.93	94°	6.82%
		νe^-	5.13	5.03	93°	2.03%
		^{12}C	36.70	35.98	93°	1.97%
$T_{\nu_e} = 3.5$ MeV	$I(1)$	$\bar{\nu}_e p$	122.28	113.93	94°	6.82%
$T_{\bar{\nu}_e} = 5$ MeV		νe^-	5.20	5.18	93°	0.36%
$T_{\nu_x} = 8$ MeV		^{12}C	39.12	38.73	93°	0.99%
$\eta_{\nu_e} = 0$	$N(0)$	$\bar{\nu}_e p$	122.28	113.93	94°	6.82%
$\eta_{\bar{\nu}_e} = 0$		νe^-	5.13	5.11	93°	0.36%
$\eta_{\nu_x} = 0$		^{12}C	39.18	38.79	93°	0.99%
	$I(0)$	$\bar{\nu}_e p$	171.72			
		νe^-	5.20			
		^{12}C	45.53			
	$N(1)$	$\bar{\nu}_e p$	163.14	151.75	95°	6.98%
		νe^-	5.13	5.00	94°	2.48%
		^{12}C	28.00	27.20	93°	2.86%
$T_{\nu_e} = 4$ MeV	$I(1)$	$\bar{\nu}_e p$	163.14	151.75	95°	6.98%
$T_{\bar{\nu}_e} = 6$ MeV		νe^-	5.13	5.11	94°	0.43%
$T_{\nu_x} = 9$ MeV		^{12}C	29.93	29.50	93°	1.43%
$\eta_{\nu_e} = 5$	$N(0)$	$\bar{\nu}_e p$	163.14	151.75	95°	6.98%
$\eta_{\bar{\nu}_e} = 2.5$		νe^-	5.13	5.11	94°	0.43%
$\eta_{\nu_x} = 2$		^{12}C	29.96	29.53	93°	1.43%
	$I(0)$	$\bar{\nu}_e p$	213.24			
		νe^-	5.13			
		^{12}C	35.16			
	$N(1)$	$\bar{\nu}_e p$	122.79	118.26	94°	3.69%
		νe^-	5.13	5.05	93°	1.59%
		^{12}C	40.58	39.93	93°	1.62%
$T_{\nu_e} = 3$ MeV	$I(1)$	$\bar{\nu}_e p$	122.79	118.26	94°	3.69%
$T_{\bar{\nu}_e} = 5$ MeV		νe^-	5.17	5.16	93°	0.21%
$T_{\nu_x} = 7$ MeV		^{12}C	43.24	42.89	92°	0.81%
$\eta_{\nu_e} = 3$	$N(0)$	$\bar{\nu}_e p$	122.79	118.26	94°	3.69%
$\eta_{\bar{\nu}_e} = 2$		νe^-	5.13	5.12	93°	0.21%
$\eta_{\nu_x} = 0$		^{12}C	43.45	43.10	92°	0.80%
	$I(0)$	$\bar{\nu}_e p$	148.53			
		νe^-	5.17			
		^{12}C	51.38			

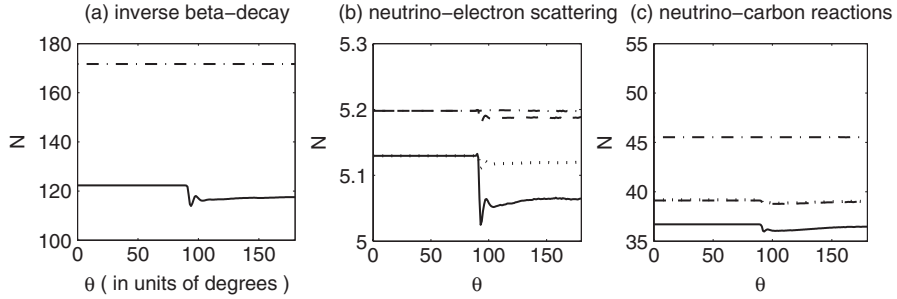

FIG. 2. The event numbers observed at the Daya Bay experiment as a function of the incident angle θ when $T_{\nu_e} = 3.5$ MeV, $T_{\bar{\nu}_e} = 5$ MeV, $T_{\nu_x} = 8$ MeV, and $\eta_{\nu_e} = \eta_{\bar{\nu}_e} = \eta_{\nu_x} = 0$. (a) the channel $\bar{\nu}_e + p \to e^+ + n$; (b) the reactions $\nu + e^- \to \nu + e^-$; (c) the neutrino-carbon reactions. The solid curves correspond to $P_H = 1$ (normal hierarchy), the dashed curves correspond to $P_H = 1$ (inverted hierarchy), the dotted curves correspond to $P_H = 0$ (normal hierarchy), and the dot-dashed curves correspond to $P_H = 0$ (inverted hierarchy). For (a), the solid curve also corresponds to $P_H = 1$ (inverted hierarchies) and $P_H = 0$ (normal hierarchy).

A. A simple case $T_{\nu_e} = 3.5$ MeV, $T_{\bar{\nu}_e} = 5$ MeV, $T_x = 8$ MeV, $\eta_{\nu_e} = \eta_{\bar{\nu}_e} = \eta_{\nu_x} = 0$

We consider, similar to Refs. [4,35], the simple case of $T_{\nu_e} = 3.5$ MeV, $T_{\bar{\nu}_e} = 5$ MeV, $T_{\nu_x} = 8$ MeV (ν_x denotes ν_μ, $\bar{\nu}_\mu$, ν_τ, or $\bar{\nu}_\tau$) and the neutrino spectra from the cooling stage to be exactly thermal, i.e., $\eta_{\nu_e} = \eta_{\bar{\nu}_e} = \eta_{\nu_x} = 0$. The realistic Earth matter density we use is given in Table I [6]. The numerical results for the event numbers for various reaction channels are given in Fig. 2.

The inverse beta-decay $\bar{\nu}_e + p \to e^+ + n$ has the largest Earth matter effect among all the channels. It can be seen from Fig. 2(a) that the maximum Earth matter effect appears at around $\theta \sim 94°$ and the effect is about 6.82% in the cases of $P_H = 0$, 1 (normal hierarchy) and $P_H = 1$ (inverted hierarchy). When the neutrino incident angle becomes larger than about 103°, the event number increases very slowly. In the case $P_H = 0$ (inverted hierarchy), the event number is independent of the incident angle.

For the neutrino-electron elastic scattering, we can see from Fig. 2(b) that the total event number is much smaller than that of the inverse beta-decay. The maximum Earth matter effect appears at $\theta \sim 93°$ and the amount is as large as 2.03% for $P_H = 1$ (normal hierarchy), 0.36% for $P_H = 1$ (inverted hierarchy), 0.36% for $P_H = 0$ (normal hierarchy), while there is no Earth matter in the case $P_H = 0$ (inverted hierarchy). When the incident angle becomes larger than about 100°, the total event numbers increase very slowly for all the above four cases. The smallness of the event number of this channel is due to the small cross sections of the neutrino-electron elastic scattering given in Eq. (3).

For the neutrino-carbon scattering, it can be seen from Fig. 2(c) that the maximum Earth matter effect appears at $\theta \sim 93°$ and the amount is as large as 1.97% for $P_H = 1$ (normal hierarchy), 0.99% for $P_H = 1$ (inverted hierarchy), 0.99% for $P_H = 0$ (normal hierarchy), while there is no Earth matter in the case $P_H = 0$ (inverted hierarchy). When the incident angle becomes larger than about 100°, the total event numbers increase slowly for all the four cases.

B. Realistic earth matter effects for different T_α and η_α

In this subsection, we consider the realistic Earth matter effects due to the variations of both the neutrino temperatures T_α and the pinching parameters η_α. In the following, we will calculate the SN neutrino event numbers for the limiting walue of T_α and η_α given in Eqs. (12) and (13). In other words, we consider the event number of SN neutrinos in the following two extreme cases:

(i) $T_{\nu_e} = 4$ MeV, $T_{\bar{\nu}_e} = 6$ MeV, $T_{\nu_x} = 9$ MeV, $\eta_{\nu_e} = 5$, $\eta_{\bar{\nu}_e} = 2.5$, $\eta_{\nu_x} = 2$;

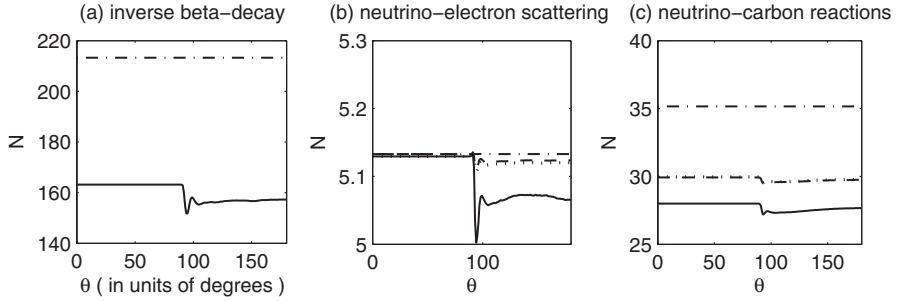

FIG. 3. Similar to Fig. 2 but T_α and η_α take their maximum values: $T_{\nu_e} = 4$ MeV, $T_{\bar{\nu}_e} = 6$ MeV, $T_{\nu_x} = 9$ MeV, $\eta_{\nu_e} = 5$, $\eta_{\bar{\nu}_e} = 2.5$, $\eta_{\nu_x} = 2$.

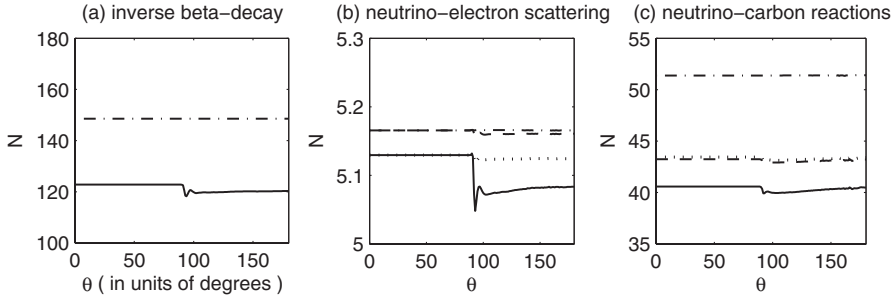

FIG. 4. Similar to Fig. 2 but T_α and η_α take their minimum values: $T_{\nu_e} = 3$ MeV, $T_{\bar{\nu}_e} = 5$ MeV, $T_{\nu_x} = 7$ MeV, $\eta_{\nu_e} = 3$, $\eta_{\bar{\nu}_e} = 2$, $\eta_{\nu_x} = 0$.

(ii) $T_{\nu_e} = 3$ MeV, $T_{\bar{\nu}_e} = 5$ MeV, $T_{\nu_x} = 7$ MeV, $\eta_{\nu_e} = 3$, $\eta_{\bar{\nu}_e} = 2$, $\eta_{\nu_x} = 0$.

The results are shown in Figs. 3 and 4.

(1) The case $T_{\nu_e} = 4$ MeV, $T_{\bar{\nu}_e} = 6$ MeV, $T_{\nu_x} = 9$ MeV, $\eta_{\nu_e} = 5$, $\eta_{\bar{\nu}_e} = 2.5$, $\eta_{\nu_x} = 2$

For the inverse beta-decay $\bar{\nu}_e + p \rightarrow e^+ + n$, it can be seen from Fig. 3(a) that the maximum Earth matter effect appears at around $\theta \sim 95°$ and the effect is about 6.98% in the cases where $P_H = 0$, 1 (normal hierarchy) and $P_H = 1$ (inverted hierarchy). When the incident angle becomes larger than about 103°, the event number increases very slowly. In the case $P_H = 0$ (inverted hierarchy), the event number is independent of the incident angle.

We can see from Fig. 3(b) that the total event number of the neutrino-electron elastic scattering is much smaller than that of the inverse beta-decay. The maximum Earth matter effect appears at $\theta \sim 94°$ and the amount is as large as 2.48% for $P_H = 1$ (normal hierarchy), 0.43% for $P_H = 1$ (inverted hierarchy), 0.43% for $P_H = 0$ (normal hierarchy), while there is no Earth matter in the case $P_H = 0$ (inverted hierarchy). When the incident angle becomes larger than about 100°, the total event numbers increase very slowly for all the above four cases.

For the neutrino-carbon scattering, it can be seen from Fig. 3(c) that the maximum Earth matter effect appears at $\theta \sim 93°$ and the amount is as large as 2.86% for $P_H = 1$ (normal hierarchy), 1.43% for $P_H = 1$ (inverted hierarchy), 1.43% for $P_H = 0$ (normal hierarchy), while there is no Earth matter in the case $P_H = 0$ (inverted hierarchy). When the incident angle becomes larger than about 100°, the total event numbers increase slowly for all the four cases.

(2) The case $T_{\nu_e} = 3$ MeV, $T_{\bar{\nu}_e} = 5$ MeV, $T_{\nu_x} = 7$ MeV, $\eta_{\nu_e} = 3$, $\eta_{\bar{\nu}_e} = 2$, $\eta_{\nu_x} = 0$

Similar to the above case, for the inverse beta-decay $\bar{\nu}_e + p \rightarrow e^+ + n$, it can be seen from Fig. 4(a) that the maximum Earth matter effect appears at around $\theta \sim 94°$ and the effect is about 3.69% in the cases where $P_H = 0$, 1 (normal hierarchy) and $P_H = 1$ (inverted hierarchy). When the incident angle becomes larger than about 103°, the event number increases very slowly. In the case $P_H = 0$ (inverted hierarchy), the event number is independent of the incident angle.

For the neutrino-electron elastic scattering, which is plotted in Fig. 4(b), the maximum Earth matter effect appears at $\theta \sim 93°$ and the amount is as large as 1.59% for $P_H = 1$ (normal hierarchy), 0.21% for $P_H = 1$ (inverted hierarchy), 0.21% for $P_H = 0$ (normal hierarchy), while there is no Earth matter in the case $P_H = 0$ (inverted hierarchy). When the incident angle becomes larger than about 100°, the total event numbers increase very slowly for all the above four cases.

Also, for the neutrino-carbon scattering, it can be seen from Fig. 4(c) that the maximum Earth matter effect appears at $\theta \sim 93°$ and the amount is as large as 1.62% for $P_H = 1$ (normal hierarchy), $\theta \sim 92°$ and 0.81% for $P_H = 1$ (inverted hierarchy), $\theta \sim 92°$ and 0.80% for $P_H = 0$ (normal hierarchy), while there is no Earth matter in the case $P_H = 0$ (inverted hierarchy). When the incident angle becomes larger than about 100°, the total event numbers increase slowly for all the four cases.

The above results can be understood by considering the fact that the oscillation behavior is determined by the factor $\triangle m^2_{21}(\mathrm{eV}^2)L(m)/E(\mathrm{MeV})$, where L is the distance that the neutrino travels in the Earth as given in Eq. (8). When $\theta < 90°$ this distance is smaller than 10 km and hence the amount of the Earth matter effects are very small. When θ increases beyond 90° this distance exceeds 100 km, the Earth matter effect becomes greater and reaches a maximum value for $91° \sim 95°$. When θ is more than 100°, the distance that neutrino travels in the Earth is greater than 2000 km, then there could be many oscillations in $F^D_{\nu_e}$ and hence the averaging Earth matter effect is smaller than the maximum value.

In Table II, we list the incipient values of the SN neutrino event numbers where the neutrino incident angle θ is zero and hence practically the vacuum event numbers,

the minimum SN neutrino event numbers and hence the maximum Earth matter effects, the incident angles at which the maximum Earth matter effects appear, and the Earth matter effects for all the cases considered. It can be seen that the realistic Earth matter effects are much smaller than those given in Ref. [4] where the mantle-core-mantle approximation for the Earth matter density was used. When both T_α and η_α vary in their ranges, the event numbers of SN neutrinos and the Earth matter effects will vary all the three reactions. More precise values of T_α and η_α will help obtain more reliable event numbers and the Earth matter effects. There are also some characters which can be seen from Table II:

(i) In the two cases: $P_H = 1$ (inverted hierarchy) and $P_H = 0$ (normal hierarchy), we have the same event numbers and the same Earth matter effects for all the three kinds of reactions;
(ii) In the case $P_H = 0$ (inverted hierarchy), the event numbers are independent of the incident angle θ (i.e. there is no Earth matter effects) for all the three kinds of reactions;
(iii) In the case $P_H = 1$ (normal hierarchies), there are the largest Earth matter effects in all the four cases for the three kinds of reactions;
(iv) When T_α and η_α increase, the maximum Earth matter effects in all the four cases increase for the three kinds of reactions.

IV. A POSSIBLE METHOD TO ACQUIRE INFORMATION ABOUT θ_{13} SMALLER THAN 1.5°

In the above section, we took the crossing probability at the high resonance region inside the SN, P_H, to be in the two extreme cases, i.e. $P_H = 0$ and $P_H = 1$, due to the fact that P_H depends on the neutrino mixing-angle θ_{13} which is unknown. In this section, using the expression of P_H, we will derive relations between the event numbers of SN neutrinos, N, and θ_{13}, and then propose a possible method to obtain information about θ_{13} smaller than 1.5°.

Considering the MSW effects [18], a number of authors including Bethe [19], Parke [20], Haxton [21], Petcov *et al.* [22], Nötzold [23], Kuo and Pantaleone [24,25] used the Landau-Zener formula [17] to calculate the crossing probability P_C at the resonance region inside a star. Several different density distributions in the case of two-flavor transitions were considered. In particular in [24,25] the following result is given:

$$P_C = \frac{\exp(-\frac{\pi}{2}\gamma F) - \exp[-\frac{\pi}{2}\gamma(\frac{F}{\sin^2\beta})]}{1 - \exp[-\frac{\pi}{2}\gamma(\frac{F}{\sin^2\beta})]}, \tag{28}$$

where β is the mixing angle and

$$\gamma = \frac{|\Delta m^2|}{2E}\frac{\sin^2 2\beta}{\cos 2\beta}\frac{1}{|d\ln N_e/dr|_{\rm res}}, \tag{29}$$

where N_e is the electron density and F can be calculated by Landau's method. The expression of F was given in Table I in Ref. [24] and Table III in Ref. [25] for different density distributions. Consequently, if we consider the following electron density distribution

$$N_e = \frac{1}{m_n + m_p}\rho \simeq \frac{1}{2m_n} k r^n, \tag{30}$$

where k is a constant and n is an integer, then

$$\gamma = \frac{1}{2|n|}\left(\frac{|\Delta m^2|}{E}\right)^{1+(1/n)}\left(\frac{\sin^2 2\beta}{\cos 2\beta}\right)\left(\frac{\cos 2\beta}{2\sqrt{2}G_F\frac{1}{2m_n}k}\right)^{1/n}, \tag{31}$$

$$F = 2\sum_{m=0}^{\infty}\binom{1/n-1}{2m}\left[\begin{matrix}1/2\\ m+1\end{matrix}\right](\tan 2\beta)^{2m}, \tag{32}$$

where

$$\begin{aligned}\binom{1/n-1}{2m} &= \frac{(1/n-1)!}{(1/n-1-2m)!(2m)!},\\ 2\left[\begin{matrix}1/2\\ m+1\end{matrix}\right] &= (-1)^m\frac{J_m - J_{m+1}}{\pi/4},\\ J_m &= \int_0^{\pi/2}(\sin\phi)^{2m}d\phi = \frac{(2m-1)!!}{(2m)!!}\frac{\pi}{2}.\end{aligned} \tag{33}$$

We note that our expression for J_m in Eq. (33) has the same final result as given in Eq. (B5) in Appendix B of Ref. [24]. But the defining integrals are different.

In order to obtain the expression for the crossing probability at the high resonance region inside the SN, P_H, we can use the similar method in the case of three-flavor transitions [26,27]. It is known that the following matter density profile for the SN is appropriate [28,43–45]:

$$\rho \approx C\cdot\left(\frac{10^7\ \text{cm}}{r}\right)^3\cdot 10^{10}\ \text{g/cm}^3, \tag{34}$$

where the constant C depends on the amount of electron capture during the star collapse and its value is between 1 and 15. This corresponds to $n = -3$ and $k = C\cdot 10^{31}$ in Eq. (30), then we have

$$\gamma = \frac{1}{6}\left[\frac{10^{10}\ \text{MeV}}{E}\left(\frac{\sin^3 2\theta_{13}}{\cos^2 2\theta_{13}}\right)\left(\frac{|\Delta m^2_{31}|}{1\ \text{eV}^2}\right)C^{1/2}\right]^{2/3}.$$

For very small θ_{13}, P_H has a simpler expression:

$$P_H = \exp\left(-\frac{\pi}{2}\gamma F\right).$$

Since θ_{13} is small, we need only to consider the $m = 0$ term in Eq. (32), then

$$F \approx 2\binom{1/n-1}{0}\left[\begin{matrix}1/2\\ 1\end{matrix}\right] = 1.$$

In addition, since $\Delta m^2_{21} \ll |\Delta m^2_{31}|$, we can set

$$|\Delta m^2_{31}| \approx |\Delta m^2_{32}|.$$

Then we obtain

$$P_H = \exp\left\{-\frac{\pi}{12}\left[\frac{10^{10}\ \text{MeV}}{E}\left(\frac{\sin^3 2\theta_{13}}{\cos^2 2\theta_{13}}\right)\times\left(\frac{|\Delta m^2_{32}|}{1\ \text{eV}^2}\right)C^{1/2}\right]^{2/3}\right\}. \quad (35)$$

In the 2σ allowed ranges [41,42,46,47]

$$|\Delta m^2_{32}| = 2.6 \times (1^{+0.14}_{-0.15}) \times 10^{-3}\ \text{eV}^2, \qquad \theta_{13} < 10°, \quad (36)$$

and we will use 2.6×10^{-3} eV^2 for $|\Delta m^2_{32}|$ in the following calculation.

From Eq. (35), the dependence of P_H on θ_{13} and E is shown explicitly. In order to obtain such simple expression of P_H, we assume θ_{13} to be very small and use the simplified structure model of SN in which $\rho \propto r^{-3}$ in the above calculations. Therefore, Eq. (35) is usually suitable for very small θ_{13} (we have checked numerically that in the range of θ_{13} we are working Eq. (35) is a good approximation), and the expression for P_H should be reevaluated if θ_{13} is larger.

In Fig. 5(a), we plot P_H as a function of θ_{13} and it can be seen that when θ_{13} is zero, $P_H = 1$; in the small range of θ_{13} of $0° \sim 2°$ P_H varies rapidly in the range $0 < P_H < 1$; and when θ_{13} is larger than $2°$, $P_H = 0$. Therefore, it is possible to use the value of P_H to obtain the value of θ_{13} when it is in the range $0° \sim 2°$. In Fig. 5(b), we plot P_H as a function of E with θ_{13} in the range $0° \sim 2°$ and again it shows that θ_{13} can be measured by the energy spectrum of P_H if the value of θ_{13} is in the range of $0° \sim 2°$.

Using Eqs. (10), (18), (21), (22), and (35), we obtain the relation between the event number of SN neutrinos N and the neutrino mixing-angle θ_{13}. The curves of N versus θ_{13} in the range $0° \sim 3°$ for the Daya Bay experiment for the inverse beta-decay is given in Fig. 6. From this plot, we can see that when $\theta_{13} \leq 1.5°$, N is very sensitive to θ_{13}. When $\theta_{13} > 1.5°$, N is nearly independent of θ_{13}. Therefore, when θ_{13} is smaller than $1.5°$, one could acquire some information about θ_{13} by detecting the event numbers of SN neutrinos. However, in practice, since we do not have the accurate values of the SN neutrino flux parameters T_α and η_α and they vary in some ranges, the event number of SN neutrinos which we will detect depend on these two unknown parameters strongly. It can be seen from Fig. 6 that the uncertainties of the event number due to those of T_α and η_α are very large, and it is difficult to obtain the value of θ_{13} from the event number of SN neutrinos. This difficulty also occurs in the neutrino-electron scattering and neutrino-carbon reactions. Therefore, we need to work with a quantity which changes with θ_{13} but is insensitive to the values of T_α and η_α.

In order to reduce uncertainties from unknown quantities such as luminosity [8], distance [40], temperatures T_α, and pinching parameters η_α, ratios of measurable quantities can be used. For instance, [48] defines the ratio of high-energy to low-energy event numbers that are measurable in neutrino oscillation experiments:

$$R = \frac{N_{\text{event}}(30 < E < 70\ \text{MeV})}{N_{\text{event}}(5 < E < 20\ \text{MeV})}. \quad (37)$$

Also, many different quantities to obtain the information about θ_{13} and the mass hierarchy are suggested in [26]. In the following we choose a suitable reaction and then define

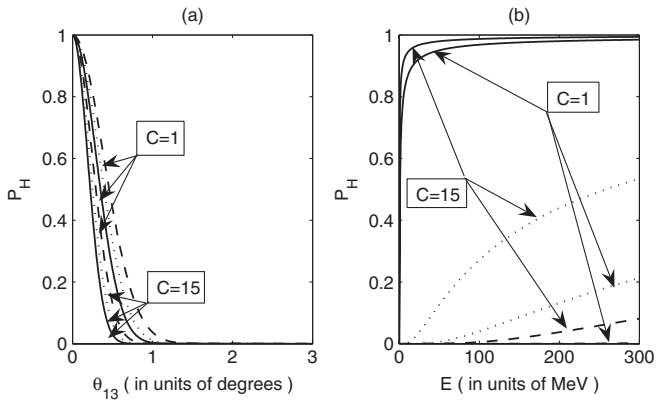

FIG. 5. The crossing probability at the high resonance region inside the SN: (a) as a function of the neutrino mixing-angle θ_{13} and the solid curves, dotted curves, dashed curves correspond to $E = 11$ MeV, 16 MeV, 25 MeV, respectively; (b) as a function of the neutrinos energy E and the solid curves, dotted curves, dashed curves correspond to $\theta_{13} = 0.1°$, $1°$, $2°$, respectively.

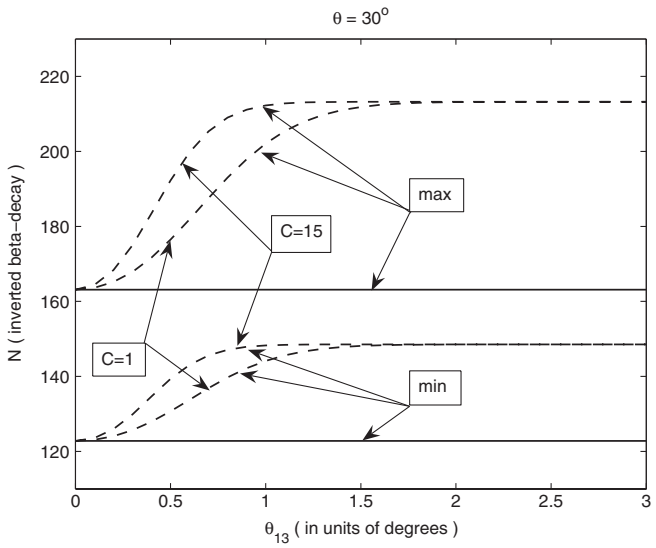

FIG. 6. The event number observed in the channel $\bar{\nu}_e + p \rightarrow e^+ + n$ at the Daya Bay experiment as a function of the neutrino mixing-angle θ_{13} when the incident angle $\theta = 30°$. The solid curves correspond to the normal hierarchy, and the dashed curves correspond to the inverted hierarchy, where "max" ("min") corresponds to the maximum (minimum) values of T_α and η_α.

a ratio of event numbers which is sensitive to the mixing-angle θ_{13} but only dependents on T_α and η_α slightly.

For the inverse beta-decay, there is only one flavor neutrino $\bar{\nu}_e$. The numerator and denominator or R of Eq. (37) have the same flavor and our calculation shows that it has a significant dependence on T_α and η_α. Hence R is not a suitable quantity to work with. In the case of neutrino-electron scattering, the event number of SN neutrinos detected at the Daya Bay experiment is very small as shown in the above section. Again this channel of reaction is not useful for our purpose. We now turn our attention to the channel of the neutrino-carbon reactions at the Daya Bay experiment.

For the neutrino-carbon reactions, we define the quantity R_1 to be the ratio which is the event number of ν_e over that of $\bar{\nu}_e$. Using Eqs. (10), (18), (21), (22), and (35), we can obtain the relation between R_1 and the mixing-angle θ_{13}. With this, we can obtain some information about θ_{13} smaller than 1.5° since the uncertainties due to T_α and η_α are small. In Fig. 7, we plot R_1 as a function of the mixing-angle θ_{13} when T_α and η_α take their limiting values in the ranges given in (12) and (13) for different incident angle θ. It can be seen from these plots that the uncertainties of R_1 due to T_α and η_α are indeed not large. For $\theta_{13} \leq 1.5°$, R_1 is very sensitive to θ_{13}. However, while $\theta_{13} > 1.5°$, R_1 is nearly independent of θ_{13}. Therefore, when θ_{13} is smaller than 1.5°, we may restrict the mixing-angle θ_{13} in a small range and get information about mass hierarchy by detecting the ratio of event numbers of SN neutrinos even though there are still some uncertainties due to the incident angle θ, the mass hierarchy $\triangle m^2_{31}$, and the structure coefficient C of the SN density function as given in Eq. (34). Recently, there are discussions on methods for the determination of the neutrino mass hierarchy and the incident angle of the SN. For examples, in Ref. [49], a method to identify the mass hierarchy at extremely small θ_{13} through the Earth matter effects is given, and a method to determine the incident angle of the SN by the electron scattering events can be found in [50]. For the structure coefficient C, its value can be more precisely determined if we can obtain more exact density profile of the SN [45]. In the future, if the incident angle θ, the mass hierarchy $\triangle m^2_{31}$, and the structure coefficient C can be determined, the uncertainties in the determination of θ_{13} through the SN neutrino will be much reduced.

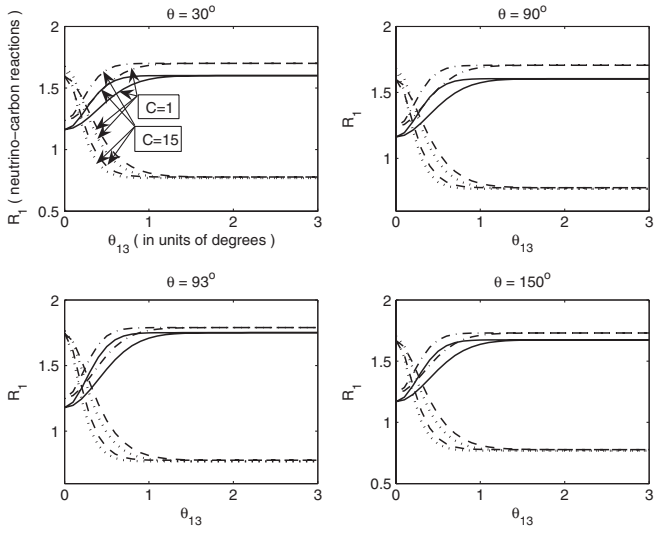

FIG. 7. The ratio of the event number of ν_e to that of $\bar{\nu}_e$, R_1, as a function of the mixing-angle θ_{13} in the channel of neutrino-carbon reactions at the Daya Bay experiment. (a) the incident angle $\theta = 30°$; (b) $\theta = 90°$; (c) $\theta = 93°$; (d) $\theta = 150°$. The solid curves correspond to the normal hierarchy (max), the dashed curves correspond to the inverted hierarchy (max), the dot-dashed curves correspond to the normal hierarchy (min), the dotted curves correspond to the inverted hierarchy (min), where "max" ("min") corresponds to the maximum (minimum) values of T_α and η_α.

At the Daya Bay experiment, the sensitivity of $\sin^2 2\theta_{13}$ will reach 0.01, i.e., to determine θ_{13} down to about 3°. Therefore, if the actual value of θ_{13} is smaller than 3°, the Daya Bay experiment can only provide an upper limit for θ_{13}. However, if an SN explosion takes place during the operation of Daya Bay, roughly within the cosmic distance considered here, it is possible to reach a much smaller value of θ_{13} through the ratio of the event number of different flavor SN neutrinos in the channel of neutrino-carbon reactions as discussed above.

V. ACQUIRING INFORMATION OF θ_{13} SMALLER THAN 1.5° FROM OTHER NEUTRINO EXPERIMENTS

In this section, we will apply the above method to some other current neutrino experiments including Super-K, SNO, KamLAND, LVD, MinBooNE, Borexino, and Double-Chooz which is under construction.

For Super-K, the target material is water, the total detector mass is 32000 tons, and the depth of the detector $h =$ 2700 m.w.e.[1] [47,48,51,52]. Then the total numbers of the targets (protons, electrons, and ^{16}O) are

$$N_T^{(p)} = 2.14 \times 10^{33}, \qquad N_T^{(e)} = 1.07 \times 10^{34}, \qquad N_T^{(O)} = 1.07 \times 10^{33}. \tag{38}$$

First, we consider the inverse beta-decay. When the incident angle $\theta = 30°$, we use Eqs. (10), (18), (21), (22), and (35) to plot the event number of SN neutrinos at Super-K as a function of the mixing-angle θ_{13}. The result is shown in Fig. 8. Similar to the Daya Bay experiment, it can be seen that the uncertainties of the event number due to the two quantities T_α and η_α are very large, and hence we cannot make predictions on θ_{13} from the event number of SN

[1] m.w.e. refers to meter-water-equivalent and 1 m of rock is about 2.7 m of water.

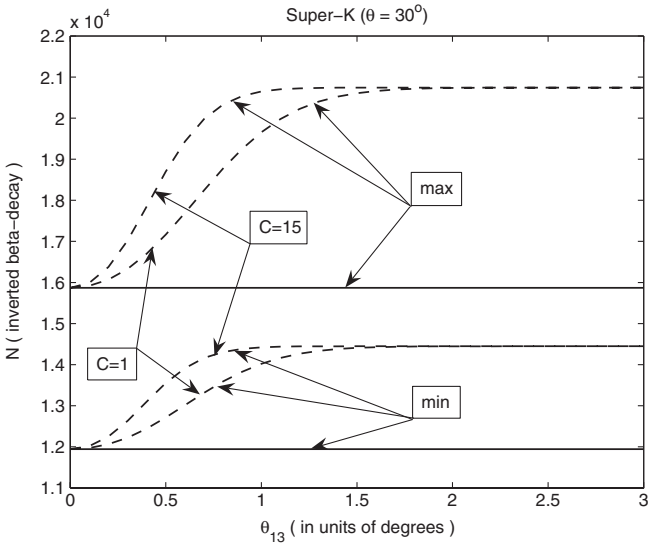

FIG. 8. Similar to Fig. 6 but for the Super-K experiment.

neutrinos. Therefore, we need to choose a suitable reaction at Super-K and find out a quantity which is sensitive to θ_{13} but only dependents on T_α and η_α slightly.

Although the event number of SN neutrinos in the channel of neutrino-electron scattering is very small at Daya Bay, it is much larger at Super-K due to the large number of target electrons $N_T^{(e)}$. We define R_2 as the ratio of the event number of ν_e to that of $\bar{\nu}_e$ from SN. Using Eqs. (10), (18), (21), (22), and (35), we can obtain the relation between R_2 and the mixing-angle θ_{13}. By measuring this ratio, we can acquire some useful information about θ_{13} smaller than 1.5° since the uncertainties due to

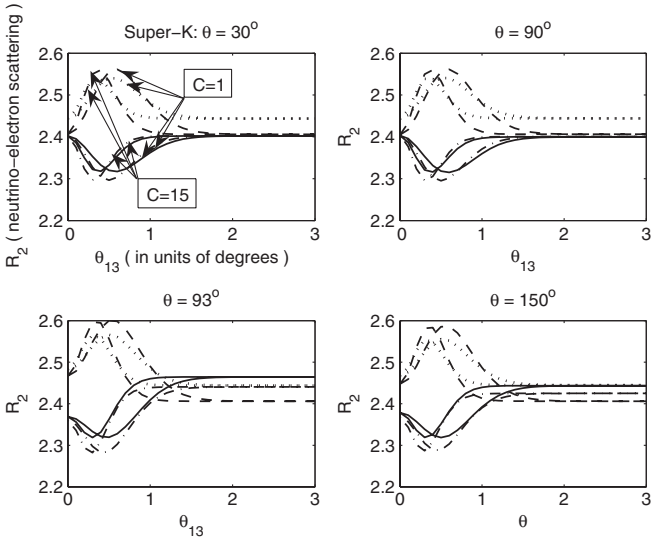

FIG. 9. Similar to Fig. 7 but for the ratio of the event number of ν_e to that of $\bar{\nu}_e$, R_2, as a function of the mixing-angle θ_{13} in the channel of neutrino-electron scattering at the Super-K experiment.

T_α and η_α are small. In Fig. 9, we plot R_2 as a function of the mixing-angle θ_{13} when T_α and η_α take their limiting values in the ranges (12) and (13) for different incident angle θ. It can be seen from these plots that the uncertainties in R_2 due to T_α and η_α are not large. When $\theta_{13} \leq 1.5°$, R_2 is very sensitive to θ_{13}. However, while $\theta_{13} > 1.5°$, R_2 is nearly independent of θ_{13}. Therefore, when θ_{13} is smaller than 1.5°, θ_{13} can be constrained in a small range by the event numbers of SN neutrinos. Furthermore, in spite of uncertainties due to θ_{13}, T_α, η_α and C, the plots show that if R_2 is smaller than about 2.35, the mass hierarchy must be normal while if R_2 is larger than about 2.5, the mass hierarchy must be inverted.

For SNO, the detector material was heavy water, the total detector mass was 1000 tons, and the depth of the detector $h = 6000$ m.w.e. [53,54]. Therefore, we need to consider the reactions between neutrinos and deuterium. There are two changed-current and six neutral-current reactions. The cross sections are obtained by scaling the experimentally measured energy values from the decay of the muon at rest to the energy scale for SN neutrinos. In this way, one can obtain [36,48,55,56]:

Charged-current capture of ν_e or $\bar{\nu}_e$:

$$\nu_e + d \rightarrow p + p + e^-, \qquad E_{\rm th} = 1.44 \text{ MeV},$$
$$\bar{\nu}_e + d \rightarrow n + n + e^+, \qquad E_{\rm th} = 4.03 \text{ MeV},$$
$$\langle\sigma(d(\nu_e, e^-)pp)\rangle = (3.35T_{\nu_e}^{2.31} - 3.70) \times 10^{-43} \text{ cm}^2,$$
$$\langle\sigma(d(\bar{\nu}_e, e^+)nn)\rangle = (3.05T_{\bar{\nu}_e}^{2.08} - 7.82) \times 10^{-43} \text{ cm}^2.$$

Neutral-current inelastic scattering of ν_α or $\bar{\nu}_\alpha$ where $\alpha = e, \mu, \tau$:

$$\nu_\alpha + d \rightarrow n + p + \nu'_\alpha, \qquad E_{\rm th} = 2.22 \text{ MeV},$$
$$\bar{\nu}_\alpha + d \rightarrow n + p + \bar{\nu}'_\alpha, \qquad E_{\rm th} = 2.22 \text{ MeV},$$
$$\langle\sigma(d(\nu_\alpha, \nu'_\alpha)np)\rangle = (1.63T_{\nu_\alpha}^{2.26} - 2.78) \times 10^{-43} \text{ cm}^2,$$
$$\langle\sigma(d(\bar{\nu}_\alpha, \bar{\nu}'_\alpha)np)\rangle = (2.03T_{\bar{\nu}_\alpha}^{2.05} - 3.76) \times 10^{-43} \text{ cm}^2.$$

For $T_{\nu_e} = 3.5$ MeV, $T_{\bar{\nu}_e} = 5$ MeV, $T_{\nu_x} = 8$ MeV,

$$\langle\sigma(d(\nu_e, e^-)pp)\rangle = 5.68 \times 10^{-42} \text{ cm}^2,$$
$$\langle\sigma(d(\bar{\nu}_e, e^+)nn)\rangle = 7.89 \times 10^{-42} \text{ cm}^2,$$
$$\langle\sigma(d(\nu_e, \nu'_\alpha)np)\rangle = 2.49 \times 10^{-42} \text{ cm}^2,$$
$$\langle\sigma(d(\bar{\nu}_e, \bar{\nu}'_\alpha)np)\rangle = 5.12 \times 10^{-42} \text{ cm}^2,$$
$$\langle\sigma(d(\nu_x, \nu'_x)np)\rangle = 1.76 \times 10^{-41} \text{ cm}^2,$$
$$\langle\sigma(d(\bar{\nu}_x, \bar{\nu}'_x)np)\rangle = 1.40 \times 10^{-41} \text{ cm}^2, \qquad x = \mu, \tau. \tag{39}$$

As indicated in Eq. (39), it can be seen that the average effective cross sections of ν_x and $\bar{\nu}_x$ reactions are different. Therefore, we need to distinguish the energy spectrum functions $F_{\nu_x}^{(0)}$ and $F_{\bar{\nu}_x}^{(0)}$ appearing in Eqs. (21) and (22).

Similar to the neutrino-carbon scattering, the average effective cross sections in Eq. (39) are given for SN neutrinos without oscillations [56]. When neutrino oscillations are taken into account, the oscillation of higher energy ν_x into ν_e again results in an increased event rate since the expected ν_e energies are just at or below the charged-current reaction threshold. This leads to an increase by a factor of 7 for the cross section $\langle\sigma(d(\nu_e, e^-)pp)\rangle$. Similarly, the cross section $\langle\sigma(d(\bar{\nu}_e, e^+)nn)\rangle$ is increased by a factor of 3. For the case of neutral-current inelastic scattering of ν_α or $\bar{\nu}_\alpha$, when the oscillation of higher energy ν_x into ν_e is taken into account, the cross section $\langle\sigma(d(\nu_e, \nu'_\alpha)np)\rangle$ is increased by a factor of 7, while when the oscillation of higher energy ν_x into $\bar{\nu}_e$ is considered, the cross section $\langle\sigma(d(\bar{\nu}_e, \bar{\nu}'_\alpha)np)\rangle$ is increased by a factor of 3.

Now, we define R_3 as the ratio of the event number of ν_e to that of $\bar{\nu}_e$ in the channel of neutrinos-deuterium scattering. Using Eqs. (10), (18), (21), (22), and (35), we can obtain the relation between R_3 and the mixing-angle θ_{13}. In Fig. 10, we plot R_3 as a function of θ_{13} when T_α and η_α take their limiting values in (12) and (13) for different incident angle θ. Similar to electron-carbon reactions, it can be seen from these plots that the uncertainties of R_3 due to T_α and η_α are not large. When $\theta_{13} \leq 1.5°$, R_3 is very sensitive to θ_{13}. However, while $\theta_{13} > 1.5°$, R_3 is nearly independent of θ_{13}. Therefore, when θ_{13} is smaller than 1.5°, we can constrain θ_{13} in a small range by the detection of the event numbers of SN neutrinos in the channel of neutrinos-deuterium reactions at SNO.

Similar to the Daya Bay experiment, the method to obtain information about θ_{13} smaller than 1.5° can be applied to KamLAND [57], LVD [58], MinBooNE [59], Borexino [60], and Double-Chooz [61] in the channel of neutrino-carbon reactions. We can also constrain θ_{13} in a small range with the ratio of the event number of SN ν_e to that of $\bar{\nu}_e$ in these experiments. Since the number of target carbons of Double-Chooz is much smaller than that of Daya Bay, the event number of SN neutrinos which can be detected is fewer and it will be more difficult to obtain information about θ_{13} by our method.

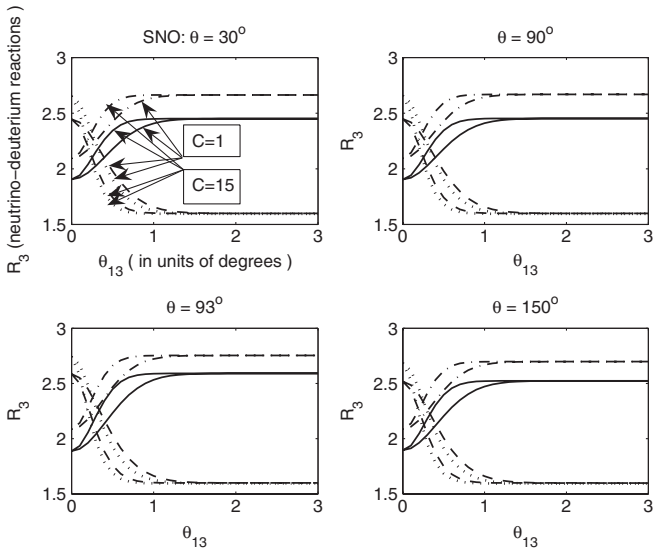

FIG. 10. Similar to Fig. 7 for the ratio of the event number of ν_e to that of $\bar{\nu}_e$, R_3, as a function of the mixing-angle θ_{13} in the channel of neutrino-deuterium reactions at the SNO experiment.

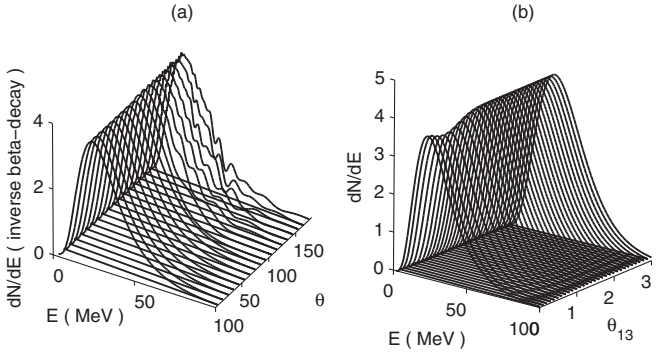

FIG. 11. In the case of inverted hierarchy, the differential event number dN/dE observed in the inverse beta-decay channel at the Daya Bay experiment as a function of the neutrino energy E. (a) for different incident angle θ ($\theta_{13} = 0$); (b) for different θ_{13} ($\theta = 30°$, $C = 3$) when $T_{\nu_e} = 3.5$ MeV, $T_{\bar{\nu}_e} = 5$ MeV, $T_{\nu_x} = 8$ MeV, $\eta_{\nu_e} = \eta_{\bar{\nu}_e} = \eta_{\nu_x} = 0$.

VI. ENERGY SPECTRA OF THE DIFFERENTIAL EVENT NUMBERS

In this section, we consider the energy spectra of the differential event numbers, referred generically as dN/dE, where E is the neutrino energy. From Eq. (10), one can obtain

$$\frac{dN_\alpha(i)}{dE} = N_T\sigma(i)\frac{1}{4\pi D^2}F_\alpha^D. \tag{40}$$

Since the inverse beta-decay is the most important reaction among the three kinds of reactions in the Daya Bay experiment, we examine the energy spectra of this process, taking the simplest parameter set $T_{\nu_e} = 3.5$ MeV, $T_{\bar{\nu}_e} = 5$ MeV, $T_{\nu_x} = 8$ MeV, $\eta_{\nu_e} = \eta_{\bar{\nu}_e} = \eta_{\nu_x} = 0$ as an example.

Using Eqs. (2), (18), (21), (22), and (40), we make a three-dimensional plot of dN/dE versus E in the Daya Bay experiment for different Earth incident angle θ in Fig. 11(a) for $\theta_{13} = 0$ (inverted hierarchy). We can see that when the incident θ increases the Earth matter effects become more and more obvious. The curve of dN/dE changing with E is very smooth when θ is small. However, it becomes oscillatory when θ is greater than 90°. Therefore, this shows that the Earth matter effects on dN/dE need to be considered in this case.

Using Eqs. (2), (18), (21), (22), (35), and (40), we plot dN/dE as a function of E for different θ_{13} in Fig. 11(b) for

the case of inverted hierarchy, where the structure coefficient of SN $C = 3$, and the Earth incident angle $\theta = 30°$ are used. We can see that the energy spectrum changes with θ_{13} in the range $0° \sim 1.5°$.

VII. SUMMARY AND DISCUSSIONS

In this paper, we have calculated the realistic Earth matter effects in the detection of type II SN neutrinos at the Daya Bay experiment under construction. It is found that the Earth matter effects depend on the neutrino incident angle θ, the neutrino mass hierarchy Δm^2_{32}, the crossing probability at the high resonance region inside the SN, P_H, the neutrino temperature T_α, the pinching parameter in the neutrino energy spectra η_α, and the collective effects of neutrino-neutrino interactions in the SN. We have given the event numbers that can be detected through the inverse beta-decay, the neutrino-electron scattering, and the neutrino-carbon scattering. We have studied the effects due to the variations of the neutrino temperature T_α and the pinching parameter η_α in the neutrino energy spectra.

Since the neutrino crossing probability at the high resonance region inside the SN, P_H, depends on the neutrino mixing-angle θ_{13}, it is possible to get information about θ_{13} by detecting SN neutrinos. In fact, there have been some general discussions on this possibility [26][29]. We have made concrete calculations and given explicit event numbers by using the relation between the event numbers of SN neutrinos N and the neutrino mixing-angle θ_{13} under different scenarios of neutrino parameters. For θ_{13} smaller than 1.5°, we propose an approach to constrain the value of angle θ_{13} in a small range and get information about mass hierarchy by measuring the ratio of the event numbers of different flavors of SN neutrinos. For the Daya Bay experiment, we choose the ratio of the event number of ν_e to that of $\bar{\nu}_e$ in the channel of neutrino-carbon reactions. We have also applied this method to other neutrino detectors including Super-K, SNO, KamLAND, LVD, MinBooNE, Borexino, and Double-Chooz. For the Super-K, the suitable reaction is the neutrino-electron scattering due to its large number of target electrons. We have also shown that the neutrino-deuterium reactions at SNO may be used to acquire useful information about θ_{13}. We stress that the measurement of θ_{13} through P_H depends on the knowledge of the primary neutrino fluxes and the density profile inside the SN.

We have studied the energy spectra of the differential event numbers, dN/dE. From the dependence of dN/dE on the neutrino energy E for different Earth incident angle θ, we have found that when the Earth incident angle θ increases the Earth matter effects become more and more pronounced.

In our calculations, we took the distance from the SN to the Earth to be 10 kpc, where the maximum of the progenitor population appears in the Milky Way [39]. The distribution of the SN progenitors as a function of the distance to the Earth can be found in Ref. [40]. It should be noted that the distance of a supernova event can be determined to a good accuracy by optical observations.

We let the parameters in the neutrino energy spectra (the temperatures and the pinching parameters) vary in some reasonable ranges. In fact, the simulations from the two leading groups, the Livermore group [34] and the Garching group [8] (which considered more reactions in their simulation and found different dominant neutrino production processes in the formation of the SN neutrino spectra and fluxes), led to parameters which agree within about 20–30%. However, their central values of SN parameters are different.

ACKNOWLEDGMENTS

We would like to thank J.-Sh. Deng, H.-L. Xiao, M.-J. Chen, K.-F. Chen, M.-H. Weng, and X.-H. Wu for helpful discussions. This work was supported in part by National Natural Science Foundation of China (Project Nos. 10535050 and 10675022), the Key Project of Chinese Ministry of Education (Project No. 106024) and the Special Grants from Beijing Normal University. B. L. Y. would like to thank Yue-Liang Wu and Jin Min Yang of the Institute of Theoretical Physics and Xin-Heng Guo of Beijing Normal University for their warm hospitality and support.

[1] K. Hirata *et al.*, Phys. Rev. Lett. **58**, 1490 (1987); R. M. Bionta *et al.*, Phys. Rev. Lett. **58**, 1494 (1987); V. Trimble, Rev. Mod. Phys. **60**, 859 (1988); W. D. Arnett, J. N. Bahcall, R. P. Kirshner, and S. E. Woosley, Annu. Rev. Astron. Astrophys. **27**, 629 (1989); W. Hillebrandt and P. Höflich, Rep. Prog. Phys. **52**, 1421 (1989).

[2] X.-H. Guo *et al.* (Daya Bay Collaboration), arXiv:hep-ex/0701029.

[3] P. Antonioli *et al.*, New J. Phys. **6**, 114 (2004).

[4] X.-H. Guo and B.-L. Young, Phys. Rev. D **73**, 093003 (2006).

[5] A. S. Dighe and A. Y. Smirnov, Phys. Rev. D **62**, 033007 (2000).

[6] A. M. Dziewonski and D. L. Anderson, Phys. Earth Planet. Inter. **25**, 297 (1981); F. D. Stacey, *Physics of the Earth* (Wiley, New York, 1977), 2nd ed..

[7] H.-T. Janka and W. Hillebrandt, Astron. Astrophys. **224**, 49 (1989); Astron. Astrophys. Suppl. Ser. **78**, 375 (1989);

H.-T. Janka, Astron. Astrophys. **244**, 378 (1991).
[8] G. G. Raffelt, Astrophys. J. **561**, 890 (2001); M. T. Keil, G. G. Raffelt, and H.-T. Janka, Astrophys. J. **590**, 971 (2003); M. T. Keil, arXiv:astro-ph/0308228; G. G. Raffelt, M. T. Keil, R. Buras, H.-T. Janka, and M. Rampp, arXiv:astro-ph/0303226.
[9] H.-Y. Duan, G. M. Fuller, J. Carlson, and Y.-Z. Qian, Phys. Rev. D **74**, 105014 (2006); Phys. Rev. Lett. **97**, 241101 (2006).
[10] G. M. Fuller and Y.-Z. Qian, Phys. Rev. D **73**, 023004 (2006); H.-Y. Duan, G. M. Fuller, and J. Carlson, J. Phys. Conf. Ser. **46**, 418 (2006); Comp. Scie. & Disc. **1**, 015007 (2008).
[11] H.-Y. Duan, G. M. Fuller, and Y.-Z. Qian, Phys. Rev. D **74**, 123004 (2006); **77**, 085016 (2008); H.-Y. Duan, G. M. Fuller, J. Carlson, and Y.-Z. Qian, Phys. Rev. D **75**, 125005 (2007); Phys. Rev. Lett. **99**, 241802 (2007); Phys. Rev. D **76**, 085013 (2007); Phys. Rev. Lett. **100**, 021101 (2008).
[12] B. Dusgupta and A. Dighe, Phys. Rev. D **77**, 113002 (2008); B. Dusgupta, A. Dighe, A. Mirizzi, and G. G. Raffelt, Phys. Rev. D **77**, 113007 (2008); **78**, 033014 (2008); S. Chakraborty, S. Choubey, B. Dasgupta, and K. Kar, J. Cosmol. Astropart. Phys. 09 (2008) 013.
[13] S. Hannestad, G. G. Raffelt, G. Sigl, and Y. Y. Wong, Phys. Rev. D **74**, 105010 (2006); **76**, 029901 (2007); G. G. Raffelt and G. Sigl, Phys. Rev. D **75**, 083002 (2007).
[14] G. G. Raffelt and A. Y. Smirnov, Phys. Rev. D **76**, 081301 (2007); **76**, 125008 (2007).
[15] A. Esteban-Pretel, S. Pastor, R. Tomàs, G. G. Raffelt, and G. Sigl, Phys. Rev. D **76**, 125018 (2007); **77**, 065024 (2008).
[16] G. L. Fogli, E. Lisi, A. Mirizzi, and D. Montanino, J. Cosmol. Astropart. Phys. 06 (2006) 012; G. L. Fogli, E. Lisi, A. Marrone, and A. Mirizzi, J. Cosmol. Astropart. Phys. 12 (2007) 010; G. L. Fogli, E. Lisi, A. Marrone, and I. Tamborra, arXiv:hep-ph/0812.3031.
[17] C. Zener, Proc. R. Soc. A **137**, 696 (1932); N. Rosen and C. Zener, Phys. Rev. **40**, 502 (1932); L. D. Landau, Phys. Z. Sowjetunion **2**, 46 (1932); L. D. Landau and E. M. Lifshitz, *Quantum Mechanics: Non-relativistic Theory* (Pergamon, New York, 1977); E. G. C. Stueckelberg, Hev. Phys. Acta. **5**, 369 (1932).
[18] L. Wolfenstein, Phys. Rev. D **17**, 2369 (1978); **20**, 2634 (1979); S. P. Mikheyev and A. Y. Smirnov, Sov. J. Nucl. Phys. **42**, 913 (1985); Nuovo Cimento C **9**, 17 (1986); Zh. Eksp. Teor. Fiz. **91**, 7 (1986); Sov. Phys. Usp. **30**, 759 (1987).
[19] H. A. Bethe, Phys. Rev. Lett. **56**, 1305 (1986).
[20] S. J. Parke, Phys. Rev. Lett. **57**, 1275 (1986).
[21] W. C. Haxton, Phys. Rev. D **35**, 2352 (1987); **36**, 2283 (1987).
[22] S. T. Petcov, Phys. Lett. B **191**, 299 (1987); **200**, 373 (1988); **214**, 139 (1988); S. T. Petcov and S. Toshev, Phys. Lett. B **187**, 120 (1987); S. Toshev, Phys. Lett. B **198**, 551 (1987); P. I. Krastev and S. T. Petcov, Phys. Lett. B **207**, 64 (1988).
[23] D. Nötzold, Phys. Rev. D **36**, 1625 (1987).
[24] T. K. Kuo and J. Pantaleone, Phys. Rev. D **39**, 1930 (1989).
[25] T. K. Kuo and J. Pantaleone, Rev. Mod. Phys. **61**, 937 (1989).
[26] C. Lunardini and A. Y. Smirnov, J. Cosmol. Astropart. Phys. 06 (2003) 009.
[27] G. L. Fogli, E. Lisi, D. Montanino, and A. Palazzo, Phys. Rev. D **65**, 073008 (2002); **66**, 013009 (2002); S. H. Chiu, Phys. Rev. D **73**, 033007 (2006); M. Kachelrieß and R. Tomàs, Phys. Rev. D **64**, 073002 (2001); M. Kachelrieß, A. Strumia, R. Tomàs, and J. W. F. Valle, Phys. Rev. D **65**, 073016 (2002); Q. Y. Liu and S. T. Petcov, Phys. Rev. D **56**, 7392 (1997); T. K. Kuo and J. Pantaleone, Phys. Rev. D **35**, 3432 (1987).
[28] K. Kotake, K. Sato, and K. Takahashi, Rep. Prog. Phys. **69**, 971 (2006).
[29] A. Dighe, J. Phys. Conf. Ser. **136**, 022041 (2008); AIP Conf. Proc. **981**, 75 (2008).
[30] C. Giunti and C. W. Kim, *Fundamentals of Neutrino Physics and Astrophysics* (Oxford, New York, 2007); S. L. Shapiro and S. A. Teukolsky, *Black Holes, White Dwarfs, and Neutron Stars* (Wiley, New York, 1983); M. Fukugita and T. Yanagida, *Physics of Neutrinos and Application to Astrophysics* (Springer, New York, 2003); R. N. Mohapatra and P. B. Pal, *Massive Neutrino in Physics and Astrophysics* (World Scientific, Singapore, 2004), 3nd ed..
[31] A. N. Ioannisian and A. Yu. Smirnov, Phys. Rev. Lett. **93**, 241801 (2004); A. N. Ioannisian, N. A. Kazarian, A. Yu. Smirnov, and D. Wyler, Phys. Rev. D **71**, 033006 (2005).
[32] C. Lunardini and A. Yu. Smirnov, Nucl. Phys. B **616**, 307 (2001); Phys. Rev. D **63**, 073009 (2001); E. K. Akhmedov, C. Lunardini, and A. Yu. Smirnov, Nucl. Phys. B **643**, 339 (2002).
[33] A. S. Dighe, M. T. Keil, and C. G. Raffelt, J. Cosmol. Astropart. Phys. 06 (2003) 006; A. S. Dighe, M. Kachelriess, C. G. Raffelt, and R. Tomas, J. Cosmol. Astropart. Phys. 01 (2004) 004; A. Mirizzi, G. G. Raffelt, and P. D. Serpico, J. Cosmol. Astropart. Phys. 05 (2006) 012.
[34] T. Totani, K. Sato, H. E. Dalhed, and J. R. Wilson, Astrophys. J. **496**, 216 (1998).
[35] L. Cadonati, F. P. Calaprice, and M. C. Chen, Astropart. Phys. **16**, 361 (2002).
[36] A. Burrows, S. Reddy, and T. A. Thompson, Nucl. Phys. A **777**, 356 (2006).
[37] A. Burrows, D. Klein, and R. Gandhi, Phys. Rev. D **45**, 3361 (1992).
[38] J. Engel, G. C. Mclaughlin, and C. Volpe, Phys. Rev. D **67**, 013005 (2003); R. Tomàs, D. Semikoz, G. G. Raffelt, M. Kachelrieß, and A. S. Dighe, Phys. Rev. D **68**, 093013 (2003).
[39] J. N. Bahcall and R. M. Soneira, Astrophys. J. Suppl. Ser. **44**, 73 (1980)J. N. Bahcall and T. Piran, Astrophys. J. **267**, L77 (1983).
[40] J. Ahrens *et al.*, Astropart. Phys. **16**, 345 (2002).
[41] G. L. Fogli, E. Lisi, A. Mirizzi, and D. Montanino, Phys. Rev. D **70**, 013001 (2004).
[42] S. Goswami, A. Bandyopadhyay, and S. Choubey, Nucl. Phys. B, Proc. Suppl. **143**, 121 (2005); G. L. Fogli, E. Lisi, D. Montanino, A. Palazzo, and A. M. Rotunno, Phys. Rev. D **69**, 017301 (2004); G. L. Fogli, E. Lisi, D. Montanino, A. Palazzo, P. Serra, J. Silk, and A. Slosar, Phys. Rev. D **75**, 053001 (2007).
[43] G. E. Brown, H. A. Bethe, and G. Baym, Nucl. Phys. A

375, 481 (1982).
[44] H. A. Bethe, Rev. Mod. Phys. **62**, 801 (1990); H. T. Janka, Astron. Astrophys. **368**, 527 (2001).
[45] S. E. Woosley and T. A. Weaver, Astrophys. J. Suppl. Ser. **101**, 181 (1995); F. X. Timmes, S. E. Woosley, and T. A. Weaver, Astrophys. J. Suppl. Ser. **98**, 617 (1995); S. E. Woosley, A. Heger, and T. A. Weaver, Rev. Mod. Phys. **74**, 1015 (2002).
[46] G. L. Fogli, E. Lisi, A. Marrone, A. Palazzo, and A. M. Rotunno, Nucl. Phys. B, Proc. Suppl. **155**, 5 (2006); M. Apollonio *et al.*, Eur. Phys. J. C **27**, 331 (2003); F. Boehm *et al.*, Phys. Rev. D **62**, 072002 (2000).
[47] Y. Fukuda *et al.*, Phys. Rev. Lett. **81**, 1562 (1998); **85**, 3999 (2000).
[48] K. Takahashi, M. Watanabe, and K. Sato, Phys. Rev. D **64**, 093004 (2001); K. Takahashi and K. Sato, Prog. Theor. Phys. **109**, 919 (2003).
[49] B. Dusgupta and A. Dighe, Phys. Rev. Lett. **101**, 171801 (2008).
[50] J. F. Beacom and P. Vogel, Phys. Rev. D **60**, 033007 (1999).
[51] J. F. Beacom and P. Vogel, Phys. Rev. D **58**, 053010 (1998); H. Yüksel, S. Ando, and J. F. Beacom, Phys. Rev. C **74**, 015803 (2006); , Phys. Rev. C **74**, 015803 (2006)
[52] Y. Fukuda *et al.*, Phys. Rev. Lett. **81**, 1158 (1998); **86**, 5651 (2001); Nucl. Instrum. Methods Phys. Res., Sect. A **501**, 418 (2003); Y. Ashie *et al.*, Phys. Rev. D **71**, 112005 (2005).
[53] J. Boger *et al.*, Nucl. Instrum. Methods Phys. Res., Sect. A **449**, 172 (2000); C. J. Virtue, Nucl. Phys. B, Proc. Suppl. **100**, 326 (2001).
[54] J. F. Beacom and P. Vogel, Phys. Rev. D **58**, 093012 (1998); J. F. Beacom and L. E. Strigari, Phys. Rev. C **73**, 035807 (2006).
[55] S. H. Chiu and T. K. Kuo, Phys. Rev. D **61**, 073015 (2000); T. A. Thompson, A. Burrows, and P. A. Pinto, Astrophys. J. **592**, 434 (2003).
[56] N. Tatara, Y. Kohyama, and K. Kubodera, Phys. Rev. C **42**, 1694 (1990); J. N. Bahcall, K. Kubodera, and S. Nozawa, Phys. Rev. D **38**, 1030 (1988); S. Ying, W. C. Haxton, and E. M. Henley, Phys. Rev. D **40**, 3211 (1989).
[57] A. Suzuki, Nucl. Phys. B, Proc. Suppl. **77**, 171 (1999); L. D. Braeckeleer, Nucl. Phys. B, Proc. Suppl. **87**, 312 (2000); J. Busenitz *et al.* (KamLAND Collaboration), Proposal for US Participation in KamLAND, March 1999; J. Busenitz, Int. J. Mod. Phys. A **16**, 742 (2001); K. Eguchi *et al.*, Phys. Rev. Lett. **90**, 021802 (2003); T. Araki *et al.*, Nature (London) **436**, 499 (2005).
[58] G. Bari *et al.*, Nucl. Instrum. Methods Phys. Res., Sect. A **277**, 11 (1989); M. Aglietta *et al.*, Nuovo Cimento**105**, 1793 (1992); W. Fulgione, Nucl. Phys. B, Proc. Suppl. **70**, 469 (1999); M. Aglietta *et al.*, Proceedings of 28th International Cosmic Ray Conferences (ICRC 2001), 1093 (2001); M. Selvi and F. Vissani, Prepared for 28th International Cosmic Ray Conferences (ICRC 2003), 1297 (2003).
[59] A. O. Bazzarko, Nucl. Phys. B, Proc. Suppl. **91**, 210 (2001); R. Tayloe, Nucl. Phys. B, Proc. Suppl. **118**, 157 (2003); S. J. Brice, Nucl. Phys. B, Proc. Suppl. **143**, 115 (2005); I. Stancu, Nucl. Phys. B, Proc. Suppl. **155**, 164 (2006); Z. Djurcic, Nucl. Phys. B, Proc. Suppl. **168**, 309 (2007); S. Case, S. Koutsoliotas, and M. L. Novak, Phys. Rev. D **65**, 077701 (2002); M. K. Sharp, J. F. Beacom, and J. A. Formaggio, Phys. Rev. D **66**, 013012 (2002).
[60] C. Galbiati, Nucl. Phys. B, Proc. Suppl. **143**, 21 (2005); G. Ranucci, Nucl. Phys. B, Proc. Suppl. **168**, 111 (2007); G. Alimonti *et al.*, Astropart. Phys. **16**, 205 (2002); M. Balata *et al.*, Eur. Phys. J. C **47**, 21 (2006).
[61] F. Ardellier *et al.*, arXiv:hep-ex/0606025; S. Berridge *et al.*, arXiv:hep-ex/0410081; M. Apollonio *et al.*, Eur. Phys. J. C **27**, 331 (2003).